



# Including the dynamic relationship between climatic variables and leaf area index in a hydrological model to improve streamflow prediction under a changing climate

Z. K. Tesemma, Y. Wei, M. C. Peel, and A. W. Western

Department of Infrastructure Engineering, The University of Melbourne, Parkville, Victoria, 3010, Australia

Correspondence to: Y. Wei (ywei@unimelb.edu.au)

Received: 25 August 2014 – Published in Hydrol. Earth Syst. Sci. Discuss.: 23 September 2014

Revised: 13 May 2015 – Accepted: 18 May 2015 – Published: 19 June 2015

**Abstract.** Anthropogenic climate change is projected to enrich the atmosphere with carbon dioxide, change vegetation dynamics and influence the availability of water at the catchment scale. This study combines a nonlinear model for estimating changes in leaf area index (LAI) due to climatic fluctuations with the variable infiltration capacity (VIC) hydrological model to improve catchment streamflow prediction under a changing climate. The combined model was applied to 13 gauged sub-catchments with different land cover types (crop, pasture and tree) in the Goulburn–Broken catchment, Australia, for the “Millennium Drought” (1997–2009) relative to the period 1983–1995, and for two future periods (2021–2050 and 2071–2100) and two emission scenarios (Representative Concentration Pathway (RCP) 4.5 and RCP8.5) which were compared with the baseline historical period of 1981–2010. This region was projected to be warmer and mostly drier in the future as predicted by 38 Coupled Model Intercomparison Project Phase 5 (CMIP5) runs from 15 global climate models (GCMs) and for two emission scenarios. The results showed that during the Millennium Drought there was about a 29.7–66.3 % reduction in mean annual runoff due to reduced precipitation and increased temperature. When drought-induced changes in LAI were included, smaller reductions in mean annual runoff of between 29.3 and 61.4 % were predicted. The proportional increase in runoff due to modeling LAI was 1.3–10.2 % relative to not including LAI. For projected climate change under the RCP4.5 emission scenario, ignoring the LAI response to changing climate could lead to a further reduction in mean annual runoff of between 2.3 and 27.7 % in the near-term (2021–2050) and 2.3 to 23.1 % later in the century (2071–2100) relative to modeling the dynamic response of

LAI to precipitation and temperature changes. Similar results (near-term 2.5–25.9 % and end of century 2.6–24.2 %) were found for climate change under the RCP8.5 emission scenario. Incorporating climate-induced changes in LAI in the VIC model reduced the projected declines in streamflow and confirms the importance of including the effects of changes in LAI in future projections of streamflow.

## 1 Introduction

Recently, climate changes have been observed in different parts of Australia (Chiew et al., 2011; Cai and Cowan, 2008; Hughes et al., 2012; Lockart et al., 2009; Potter and Chiew, 2011). Specifically, southeastern Australian catchments have experienced changes in streamflow due to fluctuations in climate as observed during the recent “Millennium Drought” (1997–2009) which lasted more than a decade (Chiew et al., 2011; Verdon-Kidd and Kiem, 2009). This drought may be representative of future climatic conditions in this region.

The projected water availability for future climates derived from downscaled outputs from global and regional climate models indicate increases of mean annual runoff by 10–40 % in some parts of the world (high northern latitudes) and 10–30 % reduction elsewhere (southern Europe, Middle East and southeastern Australia) (Milly et al., 2005). More recently, Roderick and Farquhar (2011) examined climate and catchment characteristics for sensitivity to changes in runoff in the Murray–Darling Basin in southeast Australia from a theoretical point of view and estimated that a 10 % change in precipitation would lead to a 26 % change in runoff and a

10 % change in potential evaporation would lead to a 16 % change in runoff with all other variables being constant. In southeastern Australia it has been projected that there will be a reduction in mean annual runoff of 10 % on average when different climate models are used as input to hydrological models (Cai and Cowan, 2008; Chiew et al., 2009; Roderick and Farquhar, 2011; Teng et al., 2012a; Vaze and Teng, 2011). These studies assessed the possible impacts of climate change on total runoff based on rainfall–runoff relationships which only considered first-order effects of changes in precipitation and temperature with subsequent impacts on evaporative demand.

There is evidence that such relationships are not stationary over time (Chiew et al., 2014; Peel and Blöschl, 2011; Vaze et al., 2010), which implies that the studies discussed in the previous paragraph may be missing an important factor. One approach to improving modeling under changing conditions is to use a year-to-year variable monthly leaf area index (LAI) in the hydrological model. Using observed climate variability and streamflow responses, observed monthly LAI has been shown to improve soil moisture prediction (Ford and Quiring, 2013). The improvements are largest under either relatively wet or dry climatic conditions, i.e., in wet and dry years, rather than average years. In most of southeastern Australia, LAI primarily responds to the availability of water and changes in vegetation type, such as conversion of forest to cropland or pasture, but also responds, to a lesser extent, to changes in temperature and rising atmospheric CO<sub>2</sub> concentrations. Most of these LAI responses are expected to be affected by projected climate change. These climate-induced changes in vegetation LAI may impact on evapotranspiration and runoff and hence should be considered when making runoff projections for climate change scenarios.

Dynamic global vegetation models (DGVMs) have been used to assess the vegetation effect of climate change on large-scale hydrological processes and patterns (Murray et al., 2012, 2011). A list of available DGVMs and their process representations (photosynthesis, respiration, allocation, and phenology) can be found in Wullschlegel et al. (2014), while Scheiter et al. (2013) provides a review of the possible sources of uncertainty related to representation of plant functional type (PFT) in DGVMs. Most DGVMs overestimate runoff, which is mainly due to model structure problems and operating at low spatial and temporal resolution (Murray et al., 2013). While the relationships between LAI and climatic fluctuation have been modeled (Ellis and Hatton, 2008; O'Grady et al., 2011; Jahan and Gan, 2011; Palmer et al., 2010; Tesemma et al., 2014; White et al., 2010), none of them have been incorporated into hydrological models for the purpose assessing future climate change impacts on streamflow. The poor hydrological sub-models in DGVMs and the static vegetation in most hydrological models mean that importance of the indirect vegetation-related (LAI) effects relative to the direct effects of changes in precipitation and temperature on hydrological response at catchment

scale have rarely been studied. This limits understanding of the linkages between climatic fluctuations and vegetation dynamics, and their combined impacts on hydrological processes.

The main objective of this study is to examine the relative effects on mean annual runoff of changes in direct climate forcing (mainly precipitation and temperature) and direct climate forcing combined with climate-induced LAI changes under changed climate scenarios. Comparative analysis of these two cases enables the effect on mean annual runoff of allowing LAI to respond to a changing climate to be identified. Specifically, our study combined the LAI–Climate model developed in Tesemma et al. (2014) with the Variable Infiltration Capacity (VIC) model to assess the impact on catchment runoff of how LAI is modeled (year-to-year constant monthly LAI or year-to-year variable monthly LAI in response to climate) under changing climatic conditions. As noted above, this combined model showed significant improvements in runoff simulations under historical conditions. Here we investigate two sets of changing climatic conditions: (1) the observed Millennium Drought (1997–2009), which is a persistent (> 10 years) large change in climate; and (2) projected climate change for both wet and dry catchments using 38 Coupled Model Intercomparison Project Phase 5 (CMIP5) runs from 15 different global climate models (GCMs) for two future periods, 2021–2050 and 2071–2100, for two emission scenarios, Representative Concentration Pathway (RCP) 4.5 and RCP8.5. The results obtained from this study are expected to demonstrate whether modeling LAI in a way that responds to changing climatic conditions is important for modeling runoff during projected climate change in the study area.

## 2 Research approach

This section provides details about the data set, the characteristics of the selected catchments and the modeling exercises. The catchment characteristics and data set used in this study are briefly described in Sect. 2.1. The application of multiple outputs from GCMs and emission scenario methods is explained in Sect. 2.2. The relationship between LAI and climatic variables is presented in Sect. 2.3, and the hydrological modeling experiment approach used to assess the impact of changes in climate on runoff is described in Sect. 2.4.

### 2.1 Catchment characteristics and data set

All the study sub-catchments are located in the Goulburn–Broken catchment which is a tributary of the Murray–Darling Basin, Australia. The Goulburn–Broken catchment extends between 35.8 and 37.7° S and between 144.6 and 146.7° E (Fig. 1a) with a range of altitude from approximately 1790 m on the southern side to 86 m a.m.s.l. on the northern side of the catchment. The mean annual precipi-

tation of the study sub-catchment ranges from 659 (in the north) to 1407 mm year<sup>-1</sup> (in the south) calculated for the period 1982–2012. The majority of the precipitation (about 60 %) occurs during winter and spring. The reference potential evapotranspiration (PET) calculated using the Food and Agricultural Organization (FAO56) method ranges from 903 (in the north) to 1046 mm year<sup>-1</sup> (in the south). Hence, the dryness index (mean annual reference potential evapotranspiration divided by mean annual precipitation) varies from 0.64 to 1.6 (Fig. 1b). The dominant land cover type in most of the catchments is forest (mainly tall open *Eucalyptus* forest and *Eucalyptus* woodlands) with some pasture in all catchments. A small amount of cropland is located in some of the catchments (Fig. 1c).

Gridded input data used for the hydrological modeling include the daily precipitation, maximum and minimum temperature, vapor pressure and solar exposure data obtained from the Australian Water Availability Project (AWAP) of the Bureau of Meteorology (Jones et al., 2009) and gridded daily wind run data from McVicar et al. (2008) that were generated from point measurements. All data have a spatial resolution of 0.05° × 0.05° (approximately 5 km × 5 km), and the period from 1982 to 2012 was selected for this study. The daily streamflow data at the outlet of the selected calibration sub-catchments were obtained from the Victorian Water Resources Warehouse (<http://data.water.vic.gov.au/monitoring.htm>). The missed streamflow data were filled by regressing between neighboring catchments. The elevation data were collected from the GEODATA 9 Second Digital Elevation Model (DEM-9S) Version 3 (Geoscience Australia, 2008). The elevation data were resampled to a resolution of 0.05° × 0.05° using the spatial average. The land cover input data were derived from the National Dynamic Land Cover Data set which provides a land cover map for the whole of Australia at a resolution of 0.00235° × 0.00235° (approximately 250 m × 250 m) and can be accessed at [http://www.ga.gov.au/metadata-gateway/metadata/record/gcat\\_71071](http://www.ga.gov.au/metadata-gateway/metadata/record/gcat_71071). LAI data were collected from the Global Land Surface Satellite (GLASS) product which is available for download from Beijing Normal University (<http://www.bnu-datacenter.com>). The soil parameters in the VIC model running resolution were derived from the 5' resolution Food and Agriculture Organization data set (FAO, 1995). The root distribution in three soil layers was derived from the global ecosystem root distribution data set (Schenk and Jackson, 2002).

## 2.2 Applying multiple GCMs and multiple emission scenarios

Outputs from 15 GCM from the CMIP5 (Taylor et al., 2012) were used as input into VIC model. CMIP5 contains model runs for four representative concentration pathways (RCPs), which provide radiative forcing scenarios over the 21st century (Moss et al., 2010; Vuuren et al., 2011). In this study

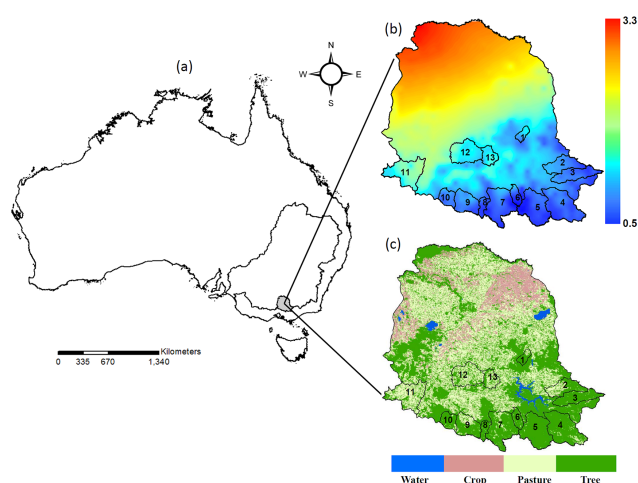


**Figure 1.** Location map of the study area (a), dryness index (mean annual reference evapotranspiration divided by mean annual precipitation) (b) and land cover type (c).

two emission scenarios were chosen: a midrange mitigation scenario, referred to as RCP4.5 and a high emissions scenario RCP8.5 (Meinshausen et al., 2011). RCP4.5 results in a radiative forcing value of 4.5 Wm<sup>-2</sup> at the end of the 21st century relative to the preindustrial value, while RCP8.5 provides a radiative forcing increase throughout the 21st century to a maximum of 8.5 Wm<sup>-2</sup> at the end of the century.

CMIP5 GCM data were obtained from <http://climexp.knmi.nl> (last accessed 28 February 2014). These data were re-sampled to a common grid resolution of 2.5° since each GCM has a different spatial resolution (some are the same, but most are different). A total of 38 RCP4.5 and 38 RCP8.5 runs from 15 different GCMs have been used in this study to include the possible uncertainty among climate models. For each of the 38 runs, daily precipitation, minimum and maximum temperature data were collected for three periods: 1981–2010 (historical run), 2021–2050 and 2071–2100 (future runs). An assessment of the ability of the CMIP5 runs to reproduce the observed baseline seasonality of precipitation, minimum and maximum temperature is shown in Fig. 2. The seasonality in precipitation and temperature were well captured by most CMIP5 runs, with biases which require correction.

Low-spatial-resolution GCM outputs require downscaling for application in catchment hydrology studies. Here the “delta-change” statistical downscaling technique was used to downscale and bias-correct the GCM outputs (Fowler et al., 2007). Delta-change was selected due to its low computational intensiveness and easy applicability to a range of GCMs. We acknowledge the limitations of this method include an assumption of stationarity in change factors, that climate feedbacks are not incorporated and an inability to capture changes in extreme events and year-to-year variability. Dynamic downscaling, which solves some of these prob-

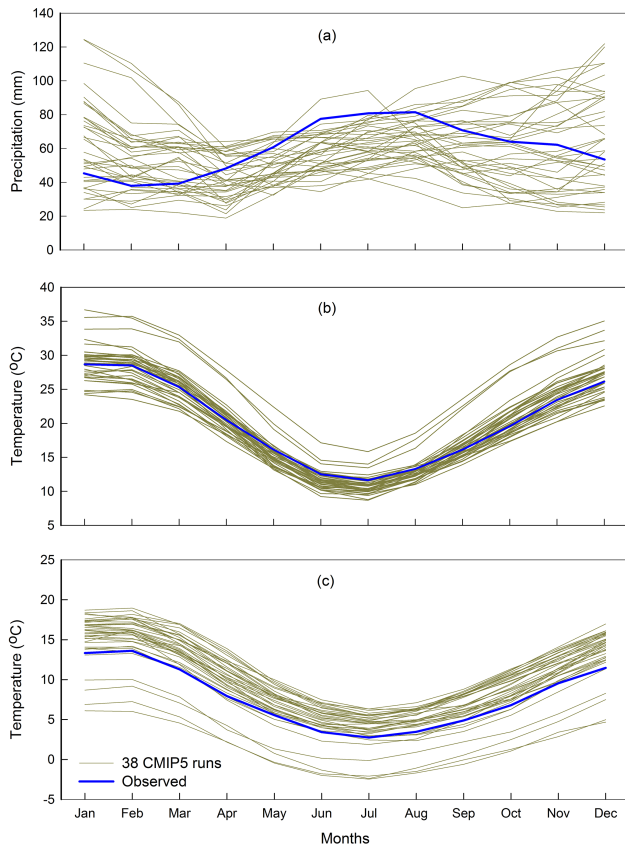


**Figure 2.** Long-term mean monthly climate observations plotted with the 38 CMIP5 runs during the baseline period (1980–2010) for the Goulburn–Broken catchment (a) long-term mean monthly precipitation, (b) long-term mean monthly maximum temperature, and (c) long-term mean monthly minimum temperature.

lems, was not used as it has high computational demand and is not readily available for a range of GCM runs and scenarios (Fowler et al., 2007). A simple statistical downscaling method was appropriate for this study as we were interested in the impact of including climate-induced LAI change on the runoff results. In the study area, the monthly LAI is strongly related to 6-month and/or 9-month moving average moisture state (precipitation minus reference potential evapotranspiration) (Tesemma et al., 2014). Therefore, so long as the precipitation is consistent between the two runs, we can assess the importance of the change in LAI representation between model runs. It has been suggested that extreme precipitation might change differently to mean precipitation under climate change (Harrold et al., 2005) and the delta-change method does not capture this. Nevertheless, delta-change was used as this study concentrates on average runoff, which is strongly linked to overall catchment wetness, rather than floods, which are linked to a combination of catchment wetness and extreme precipitation. Hence, consideration of extreme precipitation events is less important in this study.

Statistical downscaling was applied to each of the GCM outputs and emission scenarios. Since the study area is covered by four GCM grid cells, the area weighted average precipitation, minimum and maximum temperatures of the GCM grid cells covering the study area were computed. The area-weighted average values were then statistically downscaled using the delta-change approach. Delta changes were calculated separately for each of the 12 months. For temperatures the delta changes were calculated using

$$\Delta_T(j) = \bar{T}_{\text{projn}}(j) - \bar{T}_{\text{baseline}}(j), \quad (1)$$

where  $\Delta_T(j)$  is the delta change in the 30-year mean monthly minimum or maximum temperature as simulated by the climate model for the future period and RCP of interest (2021–2050 or 2071–2100, RCP4.5 or RCP8.5),  $\bar{T}_{\text{projn}}(j)$ , relative to the mean for the baseline period (1981–2010) climate model simulation,  $\bar{T}_{\text{baseline}}(j)$ .  $j$  represents the month.  $\Delta_T(j)$  is then applied to the daily baseline (1980–2010) observations,  $T_{\text{obs}}(j, i)$ , for each pixel of the climate-gridded data (which is the same as in the VIC model grid pixels) to obtain the statistically downscaled minimum or maximum daily temperature,  $T_{\Delta}(j, i)$ , for month  $j$  and day  $i$ .

$$T_{\Delta}(j, i) = T_{\text{obs}}(j, i) + \Delta_T(j) \quad (2)$$

For precipitation, the delta-changes value is computed as a proportional change rather than a shift:

$$\Delta_P(j) = \frac{\bar{P}_{\text{projn}}(j)}{\bar{P}_{\text{baseline}}(j)}. \quad (3)$$

And is then applied to the observations using

$$P_{\Delta}(j, i) = P_{\text{obs}}(j, i) \cdot \Delta_P(j). \quad (4)$$

Here  $\Delta_P(j)$  is the delta change in 30-year mean monthly precipitation as simulated by the climate model  $\bar{P}_{\text{projn}}(j)$  for two future periods (2021–2050 and 2071–2100) relative to the baseline simulation  $\bar{P}_{\text{baseline}}(j)$ ;  $P_{\Delta}(j, i)$  is the statistically downscaled daily precipitation for the projected future climate change scenario for month  $j$  and day  $i$ ,  $P_{\text{obs}}(j, i)$  is observed daily precipitation for the historical period (1981–2010) for month  $j$  and day  $i$  for each of the precipitation pixels of the gridded climate data. The delta-change approach maintains a similar (but shifted or scaled) spatial variation of temperature and precipitation as that in the historical, observed gridded data. The daily pattern of weather variation and the relationships between the various weather variables are also maintained. Because historical weather data provides the basis for the temporal patterns, the well-recognized issue of “GCM drizzle” is eliminated. The delta-change method also corrects for differences between the mean elevation of the four GCM grid cells by scaling up or down the historical spatial variation of temperature and precipitation across the catchment.

### 2.3 Relationship between LAI and climatic variables

Tesemma et al. (2014) showed that monthly LAI of each vegetation type was closely related to changes in moisture state (precipitation minus reference evapotranspiration) of 6-month moving averages for crop and pasture, and 9-month moving averages for trees. Differences in LAI response for the same change in moisture state among the three vegetation types were also observed as differences in model parameters of the LAI–Climate relationship. Tesemma et al. (2014) provide details on the derivation of the LAI–Climate relationship for the Goulburn–Broken catchment. The three LAI models developed for crop, pasture and tree are given below.

$$\text{LAI} = \begin{cases} \frac{136.4836}{1 + \exp\left(-\left(\frac{P - \text{PET} - 159.4555}{42.5607}\right)\right)}, & \text{if crop} \\ \frac{6.2495}{1 + \exp\left(-\left(\frac{P - \text{PET} - 43.6157}{62.8487}\right)\right)}, & \text{if pasture} \\ \frac{4.2091}{1 + \exp\left(-\left(\frac{P - \text{PET} + 57.1849}{36.9481}\right)\right)}, & \text{if tree,} \end{cases} \quad (5)$$

where LAI is the leaf area index of the cover type (tree/pasture/crop),  $P$  is the 6-month moving average of precipitation for crop and pasture, and the 9-month moving average for trees, and PET is the respective reference potential evapotranspiration.

The monthly LAI was then simulated for both historical and future climate scenarios using the LAI–Climate model (Eq. 5) driven with the appropriate climatic inputs. In this study monthly average PET ( $\text{mm day}^{-1}$ ) was estimated using the standard FAO Penman–Monteith daily computations (Allen et al., 1998) and then aggregating to monthly values. PET for future climate scenarios was computed using the projected minimum and maximum temperatures, while incoming shortwave radiation and vapor pressure were derived from the daily temperature range using the algorithms of Kimball et al. (1997) and Thornton and Running (1999). The wind speed was kept the same as in the historical observations. A significant literature exists (see discussion in Supplementary Material of McMahon et al., 2015) around the issue of using temperature to drive future changes in PET. We acknowledge this assumption and note that it is likely to have limited impact on our runoff results in the mainly water-limited catchments modeled here. The historical or future precipitation was used in Eq. (5) according to the scenario being modeled. Potential LAI variations in the baseline years (1981–2010) and the two future periods (2021–2050 and 2071–2100), for each of the two future emission scenarios, were simulated using the downscaled outputs from the 38 CMIP5 runs of the 15 GCMs, as input into the LAI–Climate model (Eq. 5). The uncertainty ranges in modeled LAI that come from the difference in climate input were determined by using the downscaled 38 CMIP5 runs individually in Eq. (5).

### 2.4 Hydrological model and experimental design

In this study we used the three-layers VIC model (version 4.1.2g) to simulate streamflow. The VIC macroscale model is a spatially distributed conceptual hydrological model that balances both water and energy budgets over a grid cell. It simulates soil moisture, evapotranspiration, snowpack, runoff, baseflow and other hydrological properties at daily or sub-daily time steps by solving both the governing water and energy balance equations (Liang et al., 1996). VIC estimates infiltration and runoff using the variable infiltration curve that represents the sub-grid spatial variability in soil moisture capacity (Liang et al., 1994; Zhao et al., 1980) and Penman–Monteith for potential evapotranspiration computation. The ability of the model to incorporate the spatial representation of climate and inputs of soil, vegetation and other landscape properties make it applicable for climate and land use/land cover change impact studies. The VIC model has been widely used for a number of hydrological studies in different climatic zones across the globe (Zhao et al., 2012a, b; Cuo et al., 2013).

The seven most sensitive model parameters ( $b$ ,  $D_s$ ,  $W_s$ ,  $D_{s\max}$ ,  $d_2$ ,  $d_3$  and  $\text{exp}$ ) in the VIC model (Demaria et al., 2007) were calibrated against observed streamflow from 13 selected sub-catchments with different climate and land cover composition that are representative of the main runoff generating regions of the Goulburn–Broken catchment. The model parameters were calibrated separately for each selected unregulated sub-catchment and applied uniformly within a sub-catchment (Fig. 1). The Multi-Objective Complex Evolution (MOCOM-UA) algorithm (Yapo et al., 1998) was used to calibrate the model. This algorithm was implemented on each of the selected catchments separately to calibrate the model against the observed runoff. The model was first calibrated for the entire period (1982–2012); then, using the calibrated parameters as initial guesses, the model was re-calibrated for the period 1982–1997 and evaluated for the period 1998–2012. During the calibration, VIC ran on a daily basis but the objective function was calculated on a monthly basis. Three criteria (objective functions) were used to evaluate the model's performance during calibration: the Nash–Sutcliffe efficiency (NSE) (Nash and Sutcliffe, 1970) between observed and simulated flow, the logarithm of Nash–Sutcliffe efficiency ( $\log\text{NSE}$ ) which penalizes errors at peak flow, and the percentage bias from the observed mean flow (PBIAS).

The VIC model was run at daily time steps with input data at  $5\text{ km} \times 5\text{ km}$  spatial grid resolution for 30 years, from January 1981 to December 2010, to produce the baseline run. Two model experiments were run: the first experiment considered the recent historical climate (Millennium Drought, 1997–2009) and LAI estimates using the simple LAI–Climate model against the relatively normal historical climate period (1983–1995). The second experiment considered the future climate from 38 CMIP5 runs and

corresponding LAI derivatives for two periods (2021–2050 and 2071–2100) and two emission scenarios RCP4.5 and RCP8.5 with respect to the historical period (1981–2010). Both sets of simulations were performed over the 13 calibrated sub-catchments within the Goulburn–Broken catchment (Fig. 1b). A flowchart of the modeling method is given in Fig. 3.

To identify the effect on mean annual runoff of allowing LAI to respond to a changing climate, compared with LAI not responding, we used the following steps: (1) the calibrated model was forced with inputs of historical climate data and LAI data modeled from using the historical climate data (1981–2010) to establish baseline streamflow estimates; (2) the model was forced with projected future climate inputs and corresponding modeled LAI to produce projected streamflow for future scenarios; (3) the future climates were input along with the LAI data used in step 1 to produce projected streamflow that ignores projected LAI changes. The difference in mean annual runoff between steps 3 and 1 represents the climate effect (CC effect) on mean annual runoff of only precipitation and temperature. Whereas the difference in mean annual runoff between steps 2 and 1 represents the net effect (CC + LAI effect) on mean annual runoff of allowing LAI to respond to a changing climate in addition to the direct climate forcing (precipitation and temperature). The difference in mean annual runoff between steps 2 and 3 represents the component of the runoff response related to climate-induced changes in LAI. For the Millennium Drought (1997–2009), the above two changes in mean annual runoff were estimated in a similar fashion, taking the 1983–1995 time period as a relatively normal period. The percentage change of mean annual runoff against the historical mean annual runoff for climate change effect ( $Q_{\text{clim}}$ ) (Eq. 6), climate change and LAI effect ( $Q_{\text{net}}$ ) (Eq. 7), and the percentage of CC effect offset by LAI effect ( $Q_{\text{lai}}$ ) (Eq. 8) were estimated as follows:

$$Q_{\text{clim}} = \left[ \frac{100 \cdot (Q_{\text{historical climate}}^{\text{future climate}} - Q_{\text{historical climate}}^{\text{historical LAI}})}{Q_{\text{historical LAI}}^{\text{historical climate}}} \right], \quad (6)$$

$$Q_{\text{net}} = \left[ \frac{100 \cdot (Q_{\text{future climate}}^{\text{future LAI}} - Q_{\text{historical climate}}^{\text{historical LAI}})}{Q_{\text{historical LAI}}^{\text{historical climate}}} \right], \quad (7)$$

$$Q_{\text{lai}} = \left[ \frac{100 \cdot (Q_{\text{clim}} - Q_{\text{net}})}{Q_{\text{net}}} \right]. \quad (8)$$

### 3 Results

This section provides results from the modeling exercises. First the model calibration and evaluation are discussed in Sect. 3.1. The change in climatic variables during (1) the recent observed prolonged drought and (2) future climate change projections for the study catchments are presented in Sect. 3.2. The impact on both LAI (Sect. 3.3) and catchment streamflow (Sect. 3.4) of changes in climate input during the

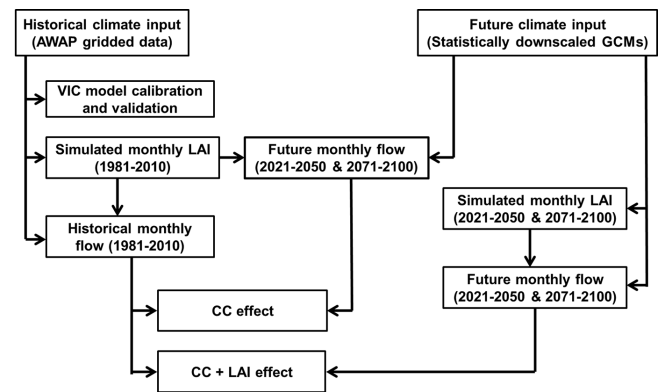


**Figure 3.** Flowchart showing the modeling experiments and calculation of effects: CC effect indicates the climate change effect of precipitation and temperature with unchanged LAI, CC + LAI effect indicates the climate change effect of precipitation, temperature and leaf area index.

Millennium Drought and future climate change projections are also provided. These results provide readers with a comparison of the anticipated future change in climate with the recently observed drought.

#### 3.1 Model calibration and evaluation results

The calibrated model parameters and model performance during calibration (1982–1997) and evaluation (1998–2012) periods for each sub-catchment are listed in Table 1. Most of the calibrated catchments have a NSE of more than 70 % during both calibration and evaluation periods (Table 1). In most of the selected sub-catchments the simulated runoff for both calibration and evaluation periods met the “satisfactory” criteria according to Moriasi et al. (2007), with a NSE > 50 % and the percentage absolute bias generally less than 25 % during calibration and evaluation periods. Although VIC captured the temporal variability of runoff well, there were some systematic biases in the runoff simulated. The model overestimates peak flow in a few cases and underestimates low flow in most of the sub-catchments. The sources of these biases need to be investigated in order to understand the performance of the model. To do this, the estimated monthly biases are plotted against the monthly climatic inputs: precipitation, temperature and LAI (not shown here). The calibrated sub-catchments showed no relationship between AWAP gridded climate data and simulated runoff biases. The biases are likely related to the model structure (Kalma et al., 1995) rather than the model inputs.



**Table 1.** Calibrated model parameters and model performance during calibration (1982–1997) and evaluation (1998–2012) periods.

ID	River and station name	Model parameters							Calibration (1982–1997)			Evaluation (1998–2012)		
		<i>b</i>	<i>D</i> <sub>s</sub>	<i>W</i> <sub>s</sub>	<i>d</i> <sub>2</sub>	<i>d</i> <sub>3</sub>	<i>D</i> <sub>smax</sub>	<i>exp</i>	Nash (%)	logNash (%)	Bias (%)	Nash (%)	logNash (%)	Bias (%)
1	Moonee Creek – Lima	0.149	0.598	0.170	1.99	0.47	0.13	2.98	82.7	80.2	2.2	86.1	78.1	8.0
2	Delatite River – Tonga Bridge	0.062	0.014	0.755	0.81	1.88	0.30	2.95	82.7	91.9	6.4	84.2	89.4	–5.4
3	Howqua River – Glen Esk	0.244	0.291	0.006	1.65	0.28	11.60	1.15	90.4	89.4	–2.5	89.3	90.3	–0.8
4	Goulburn River – Dohertys	0.206	0.891	0.035	1.43	0.45	22.01	1.42	95.9	91.0	2.2	92.4	90.8	–2.4
5	Big river – Jamieson	0.183	0.610	0.736	1.70	0.81	0.01	2.19	89.7	86.5	8.9	81.5	85.7	11.9
6	Rubicon River – Rubicon	0.216	0.059	0.200	0.52	1.77	19.29	1.28	93.8	94.9	–2.4	87.4	92.0	3.4
7	Acheron River – Taggerty	0.168	0.030	0.293	1.97	1.84	0.16	2.59	82.6	85.8	9.5	82.4	84.4	–2.4
8	Murrindindi River – above Colwells	0.130	0.801	0.297	1.97	1.89	1.11	2.67	68.9	62.8	14.6	79.7	84.7	3.9
9	Yea River – Devlins Bridge	0.072	0.428	0.646	1.93	1.27	0.05	2.99	79.8	78.3	26.4	68.0	69.3	34.1
10	King Parrot Creek – Flowerdale	0.071	0.041	0.665	0.71	1.95	0.73	2.87	61.5	66.1	45.8	73.0	62.6	41.1
11	Sugarloaf Creek – Ash Bridge	0.001	0.592	0.804	1.31	1.18	0.00	1.39	78.6	73.4	–3.5	59.0	40.0	127.5
12	Hughes Creek – Tarcombe road	0.043	0.215	0.514	1.04	1.88	0.07	3.20	82.5	89.3	9.2	62.7	58.9	39.2
13	Home Creek – Yarck	0.0004	0.415	0.524	0.66	1.91	0.01	2.97	81.7	87.1	–12.7	75.6	64.7	30.7

**Table 2.** Vegetation type distributions for each sub-catchment and changes in mean annual precipitation, temperature, LAI and streamflow during the Millennium Drought of 1997–2009 relative to 1983–1995.

Variables*	Catchments ID												
	1	2	3	4	5	6	7	8	9	10	11	12	13
Crop cover (%)	0.6	1.0	–	–	–	–	–	–	–	–	1.5	1.2	1.2
Pasture cover (%)	14.4	32.7	3.3	6.4	0.92	5.5	9.94	2.57	25.9	7.62	63.5	56.3	48.8
Tree cover (%)	85.0	66.3	96.7	93.6	99.1	94.5	90.1	97.4	74.1	92.4	35	42.6	50.1
<i>P</i> (%)	–23.2	–23.6	–21.1	–18.0	–17.9	–21.0	–20.1	–20.1	–19.4	–21.7	–19.5	–22.6	–24.1
<i>T</i> (°C)	0.2	0.3	0.3	0.4	0.4	0.3	0.3	0.2	0.3	0.2	0.3	0.3	0.3
LAI crop (%)	–44.2	–48.0	–	–	–	–	–	–	–	–	–38.1	–41.8	–41.4
LAI pasture (%)	–20.5	–21.6	–19.5	–16.9	–16.7	–18.7	–19.0	–19.1	–19.5	–19.7	–19.6	–20.2	–20.8
LAI tree (%)	–11.4	–10.3	–8.2	–6.6	–5.7	–5.9	–7.0	–6.3	–9.1	–9.2	–14.0	–12.5	–13.9
LAI total (%)	–12.9	–14.4	–8.6	–7.3	–5.8	–6.6	–8.2	–6.6	–11.8	–10.0	–17.9	–17.2	–17.6
<i>Q</i> <sub>clim</sub> (%)	–49.3	–61.5	–43.7	–39.1	–42.9	–29.7	–44.0	–41.2	–55.2	–57.1	–66.3	–61.8	–57.9
<i>Q</i> <sub>net</sub> (%)	–48.0	–59.7	–42.8	–38.3	–42.3	–29.3	–43.2	–40.6	–53.3	–55.2	–61.4	–56.1	–53.2
<i>Q</i> <sub>lai</sub> (%)	2.6	3.0	2.1	2.1	1.5	1.3	1.9	1.4	3.6	3.4	8.0	10.2	8.9

\* *P* is the change in mean annual precipitation in percentage (%), *T* is the change in mean annual temperature in degrees Celsius (°C), *Q*<sub>clim</sub> indicates the climate effect on runoff, *Q*<sub>net</sub> is the net effect of climate and LAI on runoff and *Q*<sub>lai</sub> is the proportion of the climate effect (*Q*<sub>clim</sub>) that is offset by the LAI effect.

## 3.2 Change in the climate variables from change in climate

### 3.2.1 Millennium Drought

The Millennium Drought brought a decline in the mean annual precipitation over the selected sub-catchments which ranged from 17.9 to 24.1 %, with a mean of 20.9 % when compared with the period 1983–1995. It also brought an increase in mean annual temperature which ranged from 0.2 to 0.4 °C, with an average of 0.3 °C as compared to the temperature in the period 1983–1995. All 13 study sub-catchments experienced a similar change in both precipitation and temperature (Table 2).

### 3.2.2 Future climate

Averaged over all 38 CMIP5 runs, the mean annual precipitation in 2021–2050 over the selected sub-catchments is pro-

jected to decline by 2.9 and 3.7 %, relative to the historical period 1981–2010 under the RCP4.5 and RCP8.5 scenarios respectively. By the end of the century (2071–2100) mean annual precipitation is projected to decline by 5 and 5.2 % under the RCP4.5 and RCP8.5 scenarios respectively (Table 3). The mean annual temperature is also projected to increase in both future periods and emission scenarios (Table 3).

Most precipitation projections showed a shift towards drier climates in all seasons except summer in both emission scenarios and periods. The variability in projected mean monthly precipitation among climate models indicates great uncertainty between GCMs (Fig. 4a–d). The mean monthly temperature of all climate models clearly deviated from the baseline period (1981–2010), underlining the consistent change signal between GCMs (Fig. 4e–h). The median of the 38 CMIP5 mean monthly precipitation data over the Goulburn–Broken catchment in the RCP4.5 emission scenario showed declines in most of the months. The decreases were up to 6 % in 2021–2050 (Fig. 4a) and up to 11 % in

**Table 3.** Impacts on mean annual precipitation, temperature, LAI and streamflow of projected climate change averaged over 38 CMIP5 runs relative to 1981–2010.

Periods	Variables*	Catchment ID												
		1	2	3	4	5	6	7	8	9	10	11	12	13
2021–2050 RCP4.5	<i>P</i> (%)	–2.9	–2.9	–2.9	–2.9	–2.9	–2.9	–2.9	–2.9	–2.9	–2.9	–2.9	–2.9	–2.9
	<i>T</i> (°C)	0.9	0.9	0.9	0.9	0.9	0.9	0.9	0.9	0.9	0.9	0.9	0.9	0.9
	LAI crop (%)	–12.9	–13.0	–	–	–	–	–	–	–	–	–12.9	–13.0	–12.8
	LAI pasture (%)	–5.9	–5.6	–5.4	–5.6	–5.3	–4.8	–5.4	–5.4	–6.1	–6.1	–6.7	–6.3	–6.3
	LAI tree (%)	–3.9	–2.9	–2.5	–2.4	–2.0	–1.7	–2.1	–1.9	–3.0	–3.0	–5.4	–4.6	–4.8
	LAI total (%)	–4.2	–3.9	–2.6	–2.6	–2.0	–1.8	–2.5	–1.9	–3.8	–3.2	–6.3	–5.6	–5.7
	<i>Q</i> <sub>clim</sub> (%)	–12.3	–17.6	–11.4	–11.5	–13.5	–6.8	–12.4	–12.6	–17.4	–18.4	–20.3	–18.9	–14.2
	<i>Q</i> <sub>net</sub> (%)	–11.4	–16.3	–10.9	–11.1	–13.2	–6.6	–11.9	–12.2	–15.8	–17.0	–16.3	–14.8	–11.7
	<i>Q</i> <sub>lai</sub> (%)	7.9	8.0	4.6	3.6	2.3	3.0	4.2	3.3	10.1	8.2	24.5	27.7	21.4
2021–2050 RCP8.5	<i>P</i> (%)	–3.7	–3.7	–3.7	–3.7	–3.7	–3.7	–3.7	–3.7	–3.7	–3.7	–3.7	–3.7	–3.7
	<i>T</i> (°C)	1.2	1.2	1.2	1.2	1.2	1.2	1.2	1.2	1.2	1.2	1.2	1.2	1.2
	LAI crop (%)	–15.7	–15.7	–	–	–	–	–	–	–	–	–15.7	–15.7	–15.5
	LAI pasture (%)	–7.2	–6.9	–6.7	–6.8	–6.5	–5.9	–6.6	–6.6	–7.4	–7.5	–8.1	–7.7	–7.7
	LAI tree (%)	–4.8	–3.7	–3.1	–3.0	–2.5	–2.1	–2.7	–2.3	–3.7	–3.7	–6.6	–5.6	–5.9
	LAI total (%)	–5.2	–4.8	–3.3	–3.2	–2.5	–2.3	–3.1	–2.4	–4.7	–4.0	–7.7	–6.9	–6.9
	<i>Q</i> <sub>clim</sub> (%)	–14.6	–20.7	–13.7	–13.8	–16.3	–8.3	–14.8	–15.0	–20.1	–21.3	–23.3	–21.4	–16.1
	<i>Q</i> <sub>net</sub> (%)	–13.6	–19.2	–13.2	–13.3	–15.8	–8.1	–14.3	–14.5	–18.3	–19.7	–19.0	–17.0	–13.4
	<i>Q</i> <sub>lai</sub> (%)	7.4	7.8	3.8	3.8	3.2	2.5	3.5	3.4	9.8	8.1	22.6	25.9	20.1
2071–2100 RCP4.5	<i>P</i> (%)	–5.0	–5.0	–5.0	–5.0	–5.0	–5.0	–5.0	–5.0	–5.0	–5.0	–5.0	–5.0	–5.0
	<i>T</i> (°C)	1.6	1.6	1.6	1.6	1.6	1.6	1.6	1.6	1.6	1.6	1.6	1.6	1.6
	LAI crop (%)	–21.1	–21.3	–	–	–	–	–	–	–	–	–20.8	–21.0	–20.7
	LAI pasture (%)	–9.8	–9.5	–9.2	–9.4	–9.0	–8.2	–9.2	–9.2	–10.2	–10.3	–11.0	–10.4	–10.5
	LAI tree (%)	–6.6	–5.1	–4.4	–4.2	–3.5	–3.0	–3.9	–3.4	–5.3	–5.3	–9.2	–7.8	–8.2
	LAI total (%)	–7.2	–6.7	–4.6	–4.5	–3.6	–3.3	–4.4	–3.5	–6.6	–5.7	–10.5	–9.4	–9.5
	<i>Q</i> <sub>clim</sub> (%)	–19.7	–27.5	–18.6	–18.8	–22.1	–11.5	–20.3	–20.7	–26.9	–28.1	–30.1	–27.7	–21.7
	<i>Q</i> <sub>net</sub> (%)	–18.3	–25.7	–17.9	–18.1	–21.6	–11.2	–19.6	–20.1	–24.7	–26.2	–25.2	–22.5	–18.6
	<i>Q</i> <sub>lai</sub> (%)	7.7	7.0	3.9	3.9	2.3	2.7	3.6	3.0	8.9	7.3	19.4	23.1	16.7
2071–2100 RCP8.5	<i>P</i> (%)	–5.2	–5.2	–5.2	–5.2	–5.2	–5.2	–5.2	–5.2	–5.2	–5.2	–5.2	–5.2	–5.2
	<i>T</i> (°C)	2.5	2.5	2.5	2.5	2.5	2.5	2.5	2.5	2.5	2.5	2.5	2.5	2.5
	LAI crop (%)	–28.3	–28.3	–	–	–	–	–	–	–	–	–28.5	–28.5	–28.1
	LAI pasture (%)	–13.6	–13	–12.5	–12.9	–12.2	–11.1	–12.5	–12.5	–14	–14.1	–15.4	–14.6	–14.7
	LAI tree (%)	–9.5	–7.4	–6.3	–6.0	–5.1	–4.3	–5.5	–4.8	–7.6	–7.6	–13.2	–11.2	–11.8
	LAI total (%)	–10.2	–9.4	–6.5	–6.5	–5.2	–4.7	–6.2	–5.0	–9.2	–8.1	–14.9	–13.3	–13.4
	<i>Q</i> <sub>clim</sub> (%)	–24.0	–33.5	–23.9	–24.2	–27.4	–14.5	–25.0	–25.6	–32.0	–33.0	–35.1	–32.8	–25.3
	<i>Q</i> <sub>net</sub> (%)	–22.3	–31.3	–23.0	–23.3	–26.7	–14.1	–24.0	–24.8	–29.4	–30.8	–29.2	–26.4	–21.7
	<i>Q</i> <sub>lai</sub> (%)	7.6	7.0	3.9	3.9	2.6	2.8	4.2	3.2	8.8	7.1	20.2	24.2	16.6

\* *P* is the change in mean annual precipitation in percentage (%), *T* is the change in mean annual temperature in degrees Celsius (°C), *Q*<sub>clim</sub> indicates the climate effect on runoff, *Q*<sub>net</sub> is the net effect of climate and LAI on runoff and *Q*<sub>lai</sub> is the proportion of the climate effect (*Q*<sub>clim</sub>) that is offset by the LAI effect.

2071–2100 (Fig. 4c). Similarly, under the RCP8.5 emission scenario the median monthly precipitation, other than in January and February for both periods, showed decreases of up to 7 % in 2021–2050 (Fig. 4b) and of up to 18 % in 2071–2100 (Fig. 4d). The simulations for January and February showed median increases of up to 4 and 5 % respectively in 2071–2100 from the historical baseline. Some climate models projected very wet future climates while others projected relatively dry climates. There are relatively high uncertainties in the projected mean monthly precipitation results in summer when compared with the mean monthly precipitation in winter among the climates models.

In contrast to precipitation, the projected mean monthly temperatures from all CMIP5 runs showed increases; the median of the mean monthly temperatures of all 38 CMIP5 runs increased by about 0.8 °C in winter and 1 °C in summer in

2021–2050 (Fig. 4e) and by about 1.3 °C in winter and 1.8 °C in summer in 2071–2100 (Fig. 4g) under the RCP4.5 scenario. Under the RCP8.5 emission scenario the temperatures increased by 1 °C in winter and by 1.4 °C in summer during 2021–2050 (Fig. 4f) and by 2 and 3 °C in winter and summer respectively by the end of the 21st century (Fig. 4h). After precipitation the second variable that drives water availability is potential evapotranspiration. Here PET is expected to increase among all CMIP5 runs as it is being driven solely by changes in temperature, given that actual vapor pressure and solar radiation were also simulated as a function of temperature. In the near-future period (2021–2050) the median of all CMIP5 mean monthly PET projections increase by 5–13 % in both emission scenarios, with the largest change in winter and the smallest in summer. In the future period of 2071–2100, the mean monthly PET increased by 7 % in sum-



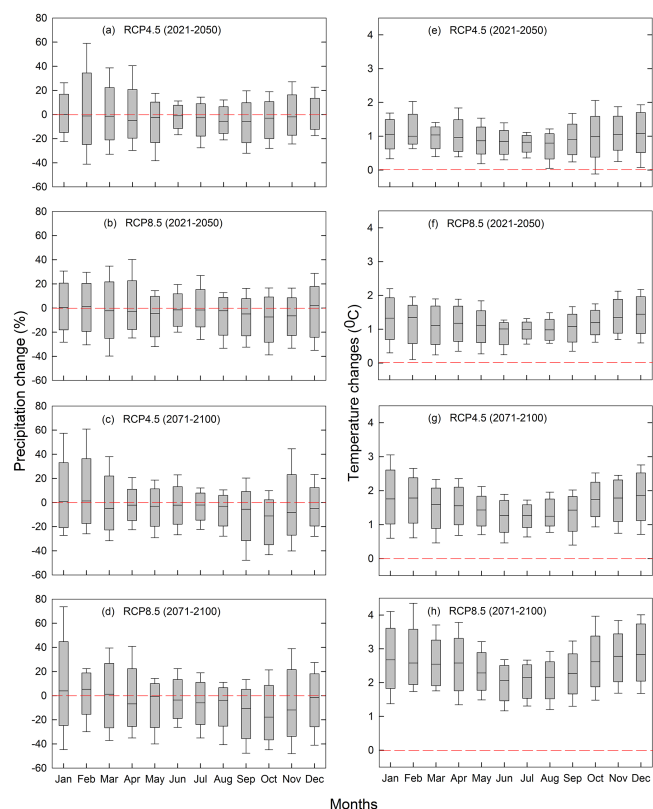


**Figure 4.** Box plots of percentage changes in the mean monthly precipitation (**a, b, c, d**) and changes in mean monthly temperatures (**e, f, g, h**) in the Goulburn–Broken catchment for the future periods 2021–2050 and 2071–2100 for the 38 CMIP5 runs of climate projections. Changes are relative to the historical (1981–2010) mean monthly precipitation and temperatures. The lower boundary of the box indicates the 25th percentile, a line within the box marks the median, the upper boundary of the box indicates the 75th percentile and the whiskers are delimited by the maximum and minimum.

mer and 25 % in winter under the RCP4.5 emission scenario, and by 10 % in summer and 28 % in winter under the RCP8.5 emission scenario.

### 3.3 Impact on LAI from change in climate

#### 3.3.1 Millennium Drought

The effects of the Millennium Drought (1997–2009) on modeled crop LAI were very severe with reductions in mean annual LAI between sub-catchments of 38.1–48.0 %, with a mean of 42.7 % (Table 2). The reduction in LAI of pasture was between 16.7 and 21.6 % across the 13 selected sub-catchments, with a spatial average of 19.4 % (Table 2). The LAI of trees responded less than crop and pasture, and reductions were in the range of 5.7–14.0 %, with a spatial mean of 9.2 % (Table 2). A significant reduction in each cover type also brought an overall decline in the areal-weighted sum of all land cover type LAIs in the selected sub-catchments,

which ranged from 5.8 to 17.9 % (Table 2), which is similar to the reduction for trees, where trees are the dominant land cover type.

#### 3.3.2 Future climate

The changes in mean monthly LAI of crop, pasture and trees averaged over the whole Goulburn–Broken catchment under future climates vary between the CMIP5 runs and global warming scenarios. Averaged over all 38 CMIP5 runs, the near-future (2021–2050) results for the study sub-catchments showed that the mean annual LAI of cropland, pasture and trees declined by up to 13, 6.7, and 5.4 % under the RCP4.5 scenario, and by up to 16, 8, and 6.6 % under the RCP8.5 scenario (Table 3). A further reduction in the mean annual LAI of each land cover was simulated by the end of the 21st century for both emission scenarios (Table 3).

The effect of projected climate change on monthly total LAI (area-weighted sum of all land cover types LAI) for the study catchment is given in (Fig. 5). The median of the 38 CMIP5-runs-simulated mean-monthly LAI showed declines in all three land cover types. Despite similar percentage changes in mean monthly precipitation and temperature forcing, the mean monthly total LAI across the catchment shows the largest decline in autumn and the smallest decline in spring during both future periods and scenarios. This difference reflects the seasonality of moisture availability influencing plant growth. Based on the median of the 38 CMIP5 runs, the predicted decline in the mean monthly LAI for crop, pasture and trees was 18.1, 10.3, and 7.9 % respectively in the period 2021–2050 (Fig. 5a, e, i) and 27.7, 16.6, and 12.8 % respectively in the period 2071–2100 under RCP4.5 (Fig. 5c, g, k). Larger reductions were simulated under the RCP8.5 emission scenario with 21.4, 12.7, and 9.5 % in the period 2021–2050 (Fig. 5b, f, j) and 36.5, 22.5, and 17.9 % respectively for crop, pasture and trees in the period 2071–2100 (Fig. 5d, h, l).

### 3.4 Impacts on runoff from change in climate

#### 3.4.1 Millennium Drought

The impact of the Millennium Drought on streamflow due to changes in precipitation and temperature alone and changes in precipitation and temperature and modeled LAI were simulated using the VIC model. The simulated reductions in mean annual streamflow during the Millennium Drought (1997–2009) as compared with the relatively normal period (1983–1995) across the selected sub-catchments due to the change in climate alone ranged from 29.7 to 66.3 %, with a mean of 50 % (Table 2). The reductions in LAI resulting from the decline in precipitation and increase in temperature increased mean annual streamflow by between 1.3 and 10.2 % relative to the direct climate effect above (Table 2, Fig. 6).

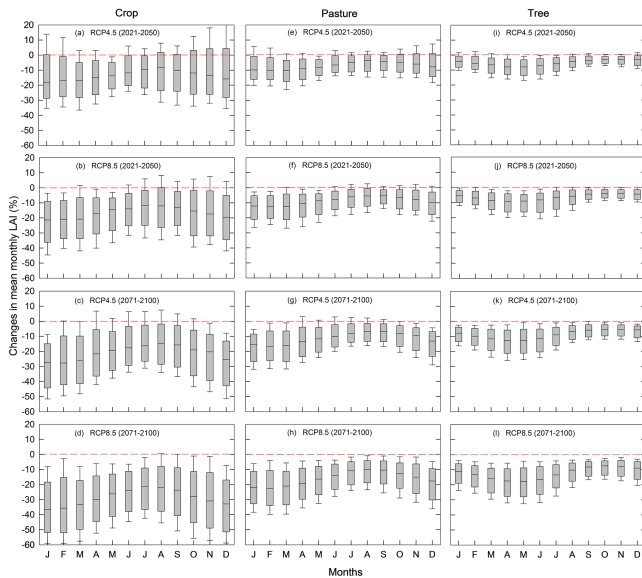


**Figure 5.** Box plots of changes in mean monthly LAI derived from the 38 CMIP5 runs for climate projections during 2021–2050 and 2071–2100 under RCP4.5 and RCP8.5 scenarios for crop (a, b, c, d), pasture (e, f, g, h) and trees (i, j, k, l) in the Goulburn–Broken catchment. Changes are relative to LAI calculated using climate time series for the 1981–2010 baseline. The lower boundary of the box indicates the 25th percentile, a line within the box marks the median, the upper boundary of the box indicates the 75th percentile and the whiskers are delimited by the maximum and minimum.

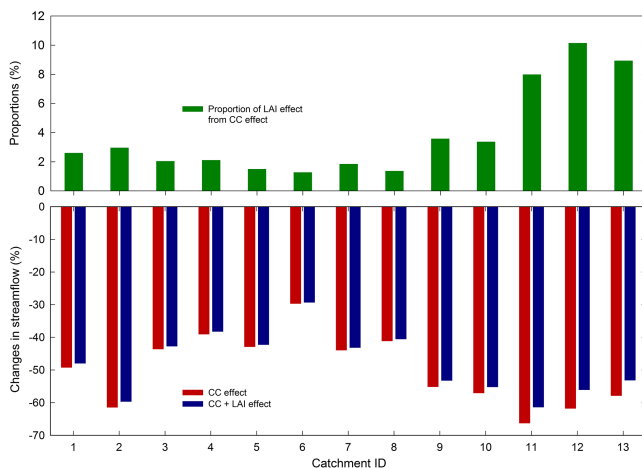


**Figure 6.** Impacts on catchment mean annual streamflow of the Millennium Drought (1997–2009) relative to the period 1983–1995. CC effect indicates precipitation and temperature effect with unchanged LAI; CC + LAI effect indicates precipitation, temperature and LAI effect. The proportional LAI effect indicates the LAI effect as a percentage of the CC effect.

### 3.4.2 Future climate

The average of the 38 CMIP5 runs under the RCP4.5 scenario produced declines in mean annual runoff due to the

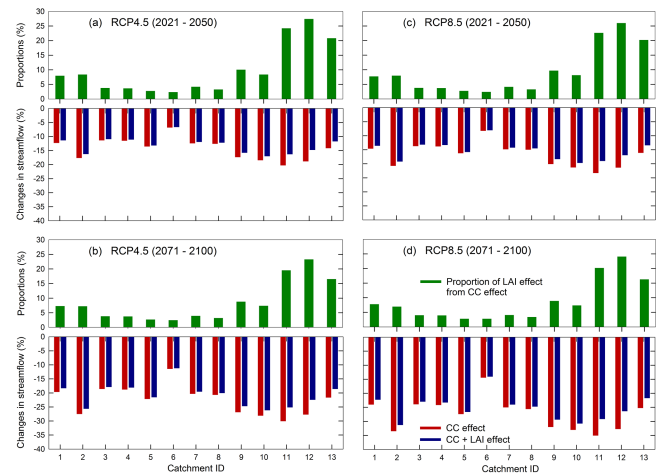


**Figure 7.** Impact on catchment mean annual streamflow average over the 38 CMIP5 runs of projected climate change for the future periods 2021–2050 and 2071–2100 under RCP4.5 (a, b) and RCP8.5 (c, d), relative to the 1981–2010 base period. CC effect indicates precipitation and temperature effect with unchanged LAI; CC + LAI effect indicates precipitation, temperature and LAI effect. The proportional LAI effect indicates the LAI effect as a percentage of the CC effect.

change in precipitation and temperature alone ( $Q_{\text{clim}}$ ), which ranged from 6.8 to 20.3 % in the period 2021–2050 and from 11.5 to 30.1 % for the period 2071–2100 (Table 3 and Fig. 7). For the higher emission scenario (RCP8.5), the reductions were a little larger ranging from 8.3 to 23.3 % in 2021–2050 and from 14.5 to 35.1 % by the end the 21st century (Table 3, Fig. 6). The reductions in runoff due to climate are offset through the LAI effect ( $Q_{\text{lai}}$ ) that ranged from 2.3 to 27.7 % and from 2.3 to 23.1 % in the near- and far-future periods respectively under the RCP4.5 emission scenario. Similar offsets of 2.5–25.9 % and 2.6–24.2 % in the near- and far-future periods respectively were also found under the RCP8.5 emission scenario (Table 3, Fig. 7).

The differences between GCMs in terms of the net climate change impacts (CC + LAI) on mean annual runoff and the LAI contribution to that effect are shown in Figs. 8 and 9 respectively. While large uncertainty exists among the 38 CMIP5 runs, the median between the models showed declines in the net climate change (CC + LAI) projections of mean annual runoff in all catchments (Fig. 8). The median decline in the mean annual runoff due to the net climate change impact was 15.3 and 26.7 % in 2021–2050 and 2071–2100 respectively, under RCP4.5. A larger decline of 21.6 and 31.8 % in 2021–2050 and 2071–2100 respectively occurred under RCP8.5 (Fig. 8). The simulated LAI effects of the climate change showed smaller variation between GCMs than the net climate change (CC + LAI) effect on mean annual runoff. The LAI effect works to offset the reduction in mean annual runoff resulting from lower precipitation and higher temperature. Figure 9 shows the magnitude of the

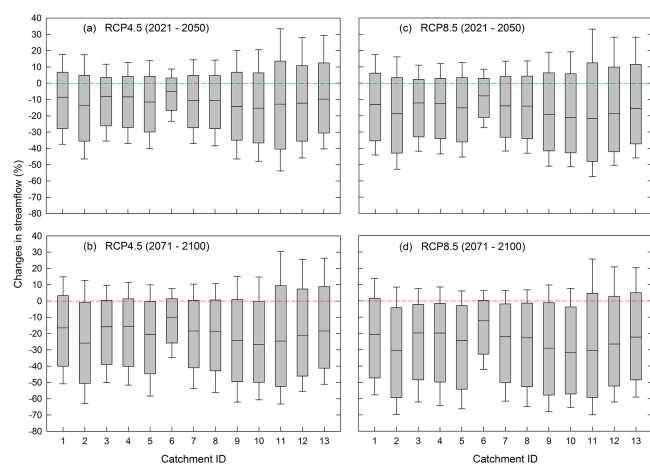


**Figure 8.** Box plots of the net climate change (CC + LAI) effect on mean annual runoff during 2021–2050 and 2071–2100 under RCP4.5 (a, b) and RCP8.5 (c, d) emission scenarios from each of the 38 CMIP5 runs. Changes are relative to the historical (1981–2010) period. The lower boundary of the box indicates the 25th percentile, a line within the box marks the median, the upper boundary of the box indicates the 75th percentile and the whiskers are delimited by the maximum and minimum.

LAI effect as a percentage of the magnitude of direct climate change effect (noting they work in opposite directions). The median of this effect across the 38 CMIP5 runs increased up to 20 %, depending on the month. The simulated LAI effect on mean annual runoff showed less variation between GCMs than the net climate change (CC + LAI) effect on mean annual runoff.

The direct climate change (CC) effect, the LAI effect of climate change and the net climate change (CC + LAI) effect on the mean monthly runoff for the selected sub-catchments are given: catchment 6 (Fig. 10a, d, g, j), catchment 10 (Fig. 10b, e, h, k), and catchment 11 (Fig. 10c, f, i, l). Catchments 6 and 10 are located in a high annual precipitation zone with trees as the dominant vegetation cover, whereas catchment 11 is covered mostly with pasture and has relatively lower annual precipitation than catchments 6 and 10. Depending on the month, for the 38 CMIP5 runs in 2021–2050 the median reduction in mean monthly runoff ( $Q_{net}$ ) was up to 10, 24, and 34 % for catchment 6, 10, and 11 respectively for both the RCP4.5 and RCP8.5 scenarios (Fig. 10). Further reductions projected by the end of the 21st century were up to 17, 37, and 52 % for catchments 6, 10, and 11 respectively under both scenarios (Fig. 10). Catchment 6 showed the lowest seasonality in the climate change effects for both emission scenarios and the LAI-related effects of climate change also showed the smallest seasonal variation. Catchment 11 runoff was the most impacted by projected climate changes and had the greatest benefit from LAI effects of climate change under both emission scenarios and future periods. The seasonal pattern of the LAI effect of climate change is similar under

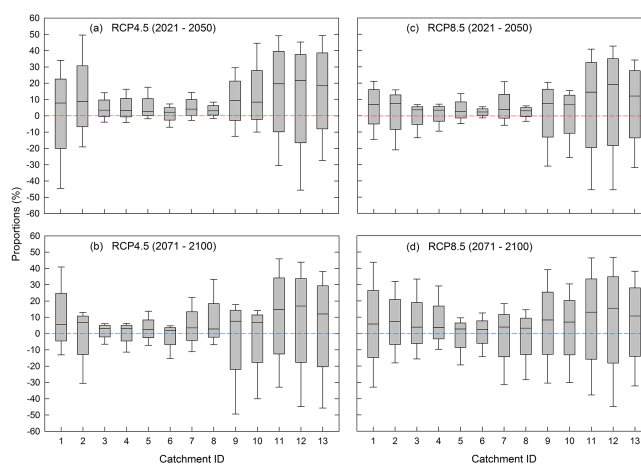


**Figure 9.** Box plots of contributions of LAI to the climate change effect on mean annual runoff for future (2021–2050, 2071–2100) climate forcings under RCP4.5 (a, b) and RCP8.5 (c, d) emission scenarios from each of the 38 CMIP5 runs as compared to the historical (1981–2010) period. The LAI effect is normalized by the effect of precipitation and temperature with unchanged LAI (i.e., CC effect) and expressed as a percentage. The lower boundary of the box indicates the 25th percentile, a line within the box marks the median, the upper boundary of the box indicates the 75th percentile and the whiskers are delimited by the maximum and minimum.

both RCP scenarios. The magnitude of this effect is relatively higher for drier projected future climates.

#### 4 Discussion and conclusion

This study investigated the importance of incorporating the relationship between changing climate, in terms of precipitation and temperature, and vegetation LAI into a hydrological model to estimate changes in mean monthly and mean annual runoff under changing climatic conditions in the Goulburn–Broken catchment, southeastern Australia. A combination of VIC hydrological simulations with a simple model that relates climatic fluctuations with LAI for three different vegetation types revealed that 21st century climate change impacts on LAI significantly influence the projected runoff in the study sub-catchments. LAIs of forest, pasture and crop were predicted to decline in the 21st century due to reductions in precipitation and increases in temperature.

Reduced LAI in response to a drier and warmer climate would reduce transpiration from vegetation and evaporative losses from canopy interception, which leaves the soil relatively wetter than if the LAI response to climate was not included. This is important for the runoff generation process as it promotes saturation excess runoff and sub-surface flow, which are the dominant cause of runoff generation in the study region (Western et al., 1999). Previous studies in the region (Chiew et al., 2009, 2011; Teng et al., 2012a, b) concluded that runoff would decrease due to increases in

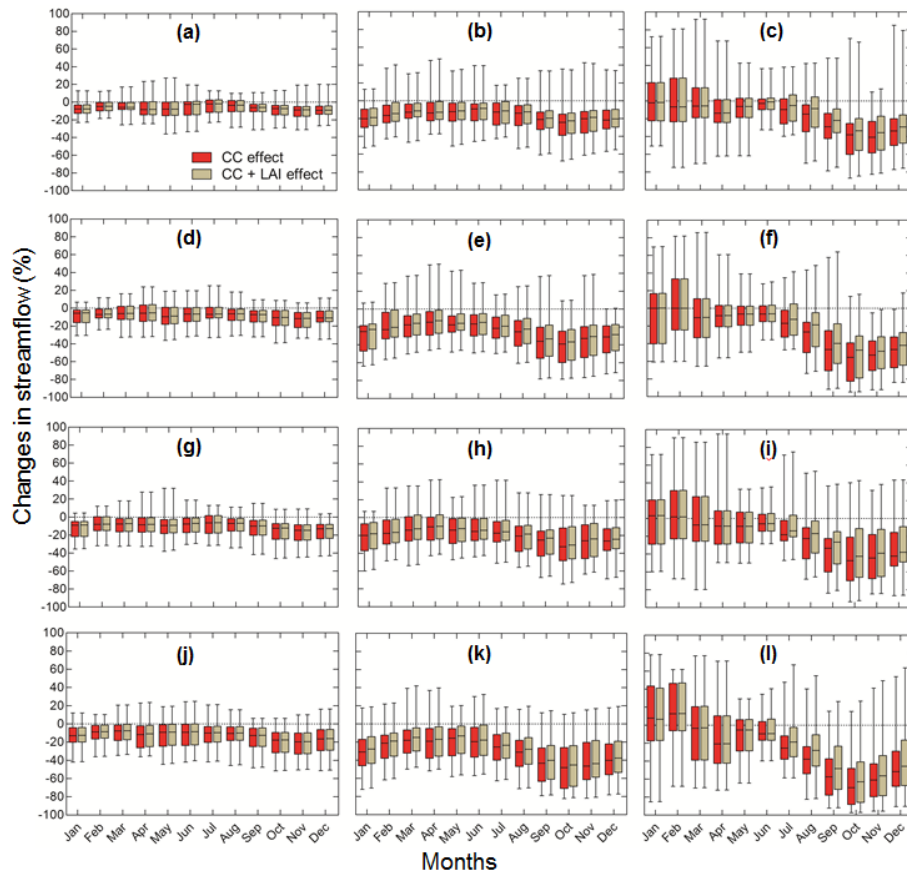


**Figure 10.** Box plots of impacts on mean monthly streamflow from 38 CMIP5 runs of catchment 6 (a, d, g and j), catchment 10 (b, e, h and k), and catchment 11 (c, f, i and l) of projected climate change for future periods 2021–2050 and 2071–2100 under RCP4.5 and RCP8.5 respectively, relative to the 1981–2010 base period. CC effect indicates precipitation and temperature effect with unchanged LAI; CC + LAI effect indicates precipitation, temperature and LAI effect. The lower boundary of the box indicates the 25th percentile, a line within the box marks the median, the upper boundary of the box indicates the 75th percentile and the whiskers are delimited by the maximum and minimum.

evaporative demand and decreases in precipitation as a result of ongoing warming in the 21st century. However, the relationship between LAI and climatic fluctuations was not taken into account in their modeling experiments. Therefore, in these studies the LAI effect is ignored and there is consequent overestimation of the runoff decline in the range of 2.3–27.7 % (Figs. 6, 7).

Projections of climate-induced vegetation dynamics and their hydrological impacts are influenced by various uncertainties that arise from using downscaled GCM outputs as inputs to the hydrological model. These include large uncertainties in projections for precipitation from the various CMIP5 simulations (Teng et al., 2012b). In addition, the method used to downscale the GCM outputs really only captures changes in the mean; however, any change in variability, which could have an effect on the projected future runoff, is ignored. The ensemble of 38 CMIP5 simulations from 15 GCMs was used to determine the range of uncertainty between GCMs. The results showed that the range of future climate projections from the various GCMs is wide, one climate

model could project a very wet future climate while another a relatively dry climate. This suggests future analyses in other catchments should apply downscaled climate change scenarios from several CMIP5 runs from a range of GCM models to the study area in order to get a sense of the possible range of climate change impact on both LAI and streamflow.

The results of this study illustrate that reduction of future precipitation and increase in mean temperature lead to reduction of runoff in a general sense. However, if the hydrological model incorporated dynamic LAI information, as a function of changing climate, it would reduce the impact on runoff that comes from the climate alone. Reduction of LAI due to reduction of precipitation and increase in temperature decreases the evapotranspiration from vegetation and leaves the soil relatively wetter than if climate-induced changes in LAI were not represented in the modeling. The higher catchment moisture contents slightly increased runoff and partially offset the reduction in runoff due to changes in climate.

In interpreting the results presented here it is important to examine the assumptions that were made and the extent

to which the results are dependent on those assumptions. Runoff processes can also be triggered by other precipitation characteristics (intensity, duration, inter-storm duration) which have not been considered in this study. If inter-storm durations are expected to increase, this will alter the hydrological fluxes even if the mean precipitation is maintained. However, the Climate–LAI model used in the study area (Tesemma et al., 2014) is related mainly to precipitation and potential evapotranspiration during the previous 6–9 months. This limits the impact of changes in extreme precipitation characteristics in terms of modeling the Climate–LAI relationship. In order to satisfy the aim of this paper, which is to assess the impact of allowing LAI to respond to a changing climate, so long as the precipitation series is consistent between the runs with and without LAI responding to climate, we can assess the importance of the change in LAI on runoff simulation. Hence, in this study, consideration of changing extreme precipitation events is less important, although it would be important for studies with the objective of predicting future floods or reservoir management.

Another assumption of this study was that the impact on runoff of rising atmospheric CO<sub>2</sub> concentrations, via changes in LAI and stomatal conductance, is small relative to the moisture availability effects. Therefore, here we assumed LAI responded only to precipitation and PET changes, not changes in CO<sub>2</sub>. Changes in atmospheric CO<sub>2</sub> concentrations could affect vegetation through increasing LAI and narrowing stomata (Ainsworth and Rogers, 2007; Ewert, 2004; Warren et al., 2011). However, increased LAI may be limited by the availability of nutrients, particularly nitrogen (Fernández-Martínez et al., 2014; Körner, 2006). Most of the results on this effect are derived from point experiments which could not be extrapolated to the catchment scale where there is a complex interaction between soil, vegetation and climate. Increasing atmospheric CO<sub>2</sub> could also have two other effects on vegetation dynamics. First, biomass allocation may shift towards more above-ground plant structure (Obrist and Arnone, 2003), which implies more canopy leaf than active rooting area. This change could influence the water balance in either direction by increasing evapotranspiration due to interception losses or by decreasing evapotranspiration through limiting plant water uptake. Second, rising atmospheric CO<sub>2</sub> may favor C<sub>3</sub> species over C<sub>4</sub> species, which could lead to more woody plants compared to some grass species (Yu et al., 2014). This could influence the water balance by increasing evapotranspiration and decreasing runoff. In addition, at the canopy scale, the evapotranspiration effect of increased LAI can be masked by shading among leaves, soil cover and raised canopy humidity (Hikosaka et al., 2005; Bunce, 2004). A study that considered both effects suggested that the fertilization effect of rising CO<sub>2</sub> is larger than the stomatal pore reduction effect, and the net effect is decreases in runoff (Piao et al., 2007). These two effects of increasing atmospheric CO<sub>2</sub> concentrations on vegetation work in opposite directions from a water balance perspective and may

offset each other if they are close in magnitude (Gerten et al., 2008). In southeast Australia, it is known that vegetation growth is highly controlled by precipitation (water supply), and is less controlled by temperature and radiation (Nemani et al., 2003). Hence, most vegetation dynamics can be explained by variation in climate, which formed the basis of the LAI–Climate model developed in Tesemma et al. (2014). We acknowledge changing CO<sub>2</sub> levels could influence vegetation growth and water use efficiency and hence runoff, but we expect the impact on runoff to be smaller (Huntington, 2008; Uddling et al., 2008) than that due to changes in moisture state. Hence, exclusion of the fertilization and stomata suppression effects of rising atmospheric CO<sub>2</sub> on vegetation may not change the results significantly. However, the impact on runoff of CO<sub>2</sub> fertilization at the catchment scale remains an important area of ongoing research.

A further assumption was that any effect of climate change on the spatial distribution of plant functional types (PFTs) was ignored. That is, the same spatial distribution of vegetation was used but with changed LAI. We acknowledge that changing climate (i.e. increase in temperature) may shift the spatial distribution of PFTs, which has been reported in the Mediterranean climate region (e.g., Lenihan et al., 2003; Crimmins et al., 2011). However, in our study area PFTs are largely determined by historical land use change (human activities), such as forest clearing for agriculture, rather than natural responses of vegetation to changed climatic conditions. Therefore, future changes in the spatial distribution of agricultural crops and pastures are difficult to project as they are not solely due to climate changes. In the forested areas, it is likely that issues that change water use such as changes in fire regime (Heath et al., 2014) and forest age (Cornish and Vertessy, 2001) would dominate over differences between species. *Eucalyptus* species already occupy high-altitude areas of the study catchment, which leaves little room for PFT changes due to upslope migration in a warming climate. Most over-story trees in our study area are *Eucalypts* and while some movement of boundaries between dominant species may be expected, water use characteristics are likely to be relatively similar, and there is insufficient information to represent species-specific details of either migration or water use. Including these effects in the model may improve the results, but there is insufficient understanding of the granularity required to do so at present.

In summary, in this paper we use the VIC hydrological model to assess the impact on mean annual streamflow of ignoring climate-induced changes in LAI for two changing climatic situations: (1) the recently observed Millennium Drought and (2) for downscaled projected future climate change scenarios from 38 CMIP5 runs in the Goulburn–Broken catchment, Australia. In the Millennium Drought (1997–2009), not modeling the response of LAI to changing climatic variables led to further reduction in mean annual runoff, relative to the pre-drought period (1983–1995), of between 1.3 and 10.2% relative to modeling the dynamic re-



sponse of LAI to decreased precipitation and increased temperature (Table 2, Fig. 6). For projected climate change under the RCP4.5 emission scenario, ignoring the LAI response to changing climate could lead to a further reduction in mean annual runoff of between 2.3 and 27.7 %, relative to the baseline period (1981–2010), in the near-term (2021–2050) and 2.3–23.1 % later in the century (2071–2100), relative to modeling the dynamic response of LAI to precipitation and temperature changes. Similar results (near-term 2.5–25.9 % and end-of-century 2.6–24.2 %) were found for climate change under the RCP8.5 emission scenario (Table 3, Fig. 7). Due to the strong relationship between climatic variation and LAI, the Climate–LAI interaction should be included in hydrological models for improved climate change impact assessments and modeling under changing climatic conditions, particularly in arid and semi-arid regions where vegetation is strongly influenced by climate.

*Acknowledgements.* This study was funded by the Australian Research Council (ARC) (project no: ARC LP100100546, ARC FT130100274 and ARC FT120100130), the Natural Science Foundation of China (project no: 91125007) and the Commonwealth of Australia under the Australia China Science and Research Fund (project no: ACSRF800). We would like to thank the University of Melbourne for providing a scholarship to the first author. We thank editor Ciaran Harman and two anonymous reviewers for comments that improved this manuscript.

Edited by: C. Harman

## References

- Ainsworth, E. A. and Rogers, A.: The response of photosynthesis and stomatal conductance to rising [CO<sub>2</sub>]: mechanisms and environmental interactions, *Plant Cell Environ.*, 30, 258–270, doi:10.1111/j.1365-3040.2007.01641.x, 2007.
- Allen, R. G., Pereira, L. S., Raes, D., and Smith, M.: Crop evapotranspiration Guidelines for computing crop water requirements, FAO Irrigation and Drainage Paper 56, Food and Agriculture Organization of the United Nations, 1998.
- Bunce, J. A.: Carbon dioxide effects on stomatal responses to the environment and water use by crops under field conditions, *Oecologia*, 140, 1–10, doi:10.1007/s00442-003-1401-6, 2004.
- Cai, W. and Cowan, T.: Evidence of impacts from rising temperature on inflows to the Murray–Darling Basin, *Geophys. Res. Lett.*, 35, L07701, doi:10.1029/2008GL033390, 2008.
- Chiew, F. H. S., Teng, J., Vaze, J., Post, D. A., Perraud, J. M., Kirono, D. G. C., and Viney, N. R.: Estimating climate change impact on runoff across southeast Australia: method, results, and implications of the modeling method, *Water Resour. Res.*, 45, W10414, doi:10.1029/2008WR007338, 2009.
- Chiew, F. H. S., Young, W. J., Cai, W., and Teng, J.: Current drought and future hydroclimate projections in southeast Australia and implications for water resources management, *Stoch. Environ. Res. Risk A.*, 25, 601–612, doi:10.1007/s00477-010-0424-x, 2011.
- Chiew, F. H. S., Potter, N. J., Vaze, J., Petheram, C., Zhang, L., Teng, J., and Post, D. A.: Observed hydrologic non-stationarity in far south-eastern Australia: implications for modelling and prediction, *Stoch. Environ. Res. Risk A.*, 28, 3–15, 2014.
- Cornish, P. M. and Vertessy, R. A.: Forest age-induced changes in evapotranspiration and water yield in a eucalypt forest, *J. Hydrol.*, 242, 43–63, doi:10.1016/S0022-1694(00)00384-X, 2001.
- Crimmins, S. M., Dobrowski, S. Z., Greenberg, J. A., Abatzoglou, J. T., and Mynsberge, A. R.: Changes in climatic water balance drive downhill shifts in plant species' optimum elevations, *Science*, 331, 324–327, 2011.
- Cuo, L., Zhang, Y., Gao, Y., Hao, Z., and Cairang, L.: The impacts of climate change and land cover/use transition on the hydrology in the upper Yellow River Basin, China, *J. Hydrol.*, 502, 37–52, doi:10.1016/j.jhydrol.2013.08.003, 2013.
- Demaria, E. M., Nijssen, B., and Wagener, T.: Monte Carlo sensitivity analysis of land surface parameters using the Variable Infiltration Capacity model, *J. Geophys. Res.*, 112, D11113, doi:10.1029/2006JD007534, 2007.
- Ellis, T. W. and Hatton, T. J.: Relating leaf area index of natural eucalypt vegetation to climate variables in southern Australia, *Agr. Water Manage.*, 95, 743–747, doi:10.1016/j.agwat.2008.02.007, 2008.
- Ewert, F.: Modelling plant responses to elevated CO<sub>2</sub>: how important is leaf area index?, *Ann. Bot.*, 93, 619–627, doi:10.1093/aob/mch101, 2004.
- Food and Agriculture Organization of the United Nations (FAO): Digital soil map of the world, Version 3.5. FAO, Rome, Italy, 1995.
- Fernández-Martínez, M., Vicca, S., Janssens, I., Sardans, J., Luysaert, S., Campioli, M., Chapin III, F., Ciais, P., Malhi, Y., and Obersteiner, M.: Nutrient availability as the key regulator of global forest carbon balance, *Nature Climate Change*, 4, 471–476, 2014.
- Fowler, H. J., Blenkinsop, S., and Tebaldi, C.: Linking climate change modelling to impacts studies: recent advances in down-scaling techniques for hydrological modelling, *Int. J. Climatol.*, 27, 1547–1578, doi:10.1002/joc.1556, 2007.
- Ford, T. W. and Quiring, S. M.: Influence of MODIS-Derived Dynamic Vegetation on VIC-Simulated Soil Moisture in Oklahoma, *J. Hydrometeorol.*, 14, 1910–1921, doi:10.1175/JHM-D-13-037.1, 2013.
- Geoscience Australia: GEODATA 9 Second Digital Elevation Model (DEM-9S) Version 3, available at: [http://www.ga.gov.au/metadata-gateway/metadata/record/gcat\\_66006](http://www.ga.gov.au/metadata-gateway/metadata/record/gcat_66006), last access: 20 December 2013, 2008.
- Gerten, D., Rost, S., von Bloh, W., and Lucht, W.: Causes of change in 20th century global river discharge, *Geophys. Res. Lett.*, 35, L20405, doi:10.1029/2008GL035258, 2008.
- Harrold, T. I., Jones, R. N., and Watterson, I. G.: Applying climate changes simulated by GCMs to the generation of fine-scale rainfall scenarios, *Hydro 2005, 29th Hydrology and Water Resources Symposium*, Canberra, 2005.
- Heath, J. T., Chafer, C. J., van Ogtrop, F. F., and Bishop, T. F. A.: Post-wildfire recovery of water yield in the Sydney Basin water supply catchments: An assessment of the 2001/2002 wildfires, *J. Hydrol.*, 519, 1428–1440, doi:10.1016/j.jhydrol.2014.09.033, 2014.



- Hikosaka, K., Onoda, Y., Kinugasa, T., Nagashima, H., Anten, N. P. R., and Hirose, T.: Plant responses to elevated CO<sub>2</sub> concentration at different scales: leaf, whole plant, canopy, and population, *Ecol. Res.*, 20, 243–253, doi:10.1007/s11284-005-0041-1, 2005.
- Hughes, J. D., Petrone, K. C., and Silberstein, R. P.: Drought, groundwater storage and stream flow decline in south-western Australia, *Geophys. Res. Lett.*, 39, L03408, doi:10.1029/2011GL050797, 2012.
- Huntington, T. G.: CO<sub>2</sub>-induced suppression of transpiration cannot explain increasing runoff, *Hydrol. Process.*, 22, 311–314, doi:10.1002/hyp.6925, 2008.
- Jahan, N. and Gan, T. Y.: Modelling the vegetation–climate relationship in a boreal mixedwood forest of Alberta using normalized difference and enhanced vegetation indices, *Int. J. Remote Sens.*, 32, 313–335, doi:10.1080/01431160903464146, 2011.
- Jones, D. A., Wang, W., and Fawcett, R.: High-quality spatial climate data-sets for Australia, *Australian Meteorological and Oceanographic Journal*, 58, 233–248, 2009.
- Kalma, J. D., Bates, B. C., and Woods, R. A.: Predicting catchment-scale soil moisture status with limited field measurements, *Hydrol. Process.*, 9, 445–467, doi:10.1002/hyp.3360090315, 1995.
- Kimball, J. S., Running, S. W., and Nemani, R. R.: An improved method for estimating surface humidity from daily minimum temperature, *Agr. Forest Meteorol.*, 85, 87–98, 1997.
- Körner, C.: Plant CO<sub>2</sub> responses: an issue of definition, time and resource supply, *New Phytol.*, 172, 393–411, doi:10.1111/j.1469-8137.2006.01886.x, 2006.
- Lenihan, J. M., Drapek, R., Bachelet, D., and Neilson, R. P.: Climate change effects on vegetation distribution, carbon, and fire in California, *Ecol. Appl.*, 13, 1667–1681, 2003.
- Liang, X., Lettenmaier, D. P., Wood, E. F., and Burges, S. J.: A Simple hydrologically based model of land surface water and energy fluxes of general circulation models, *J. Geophys. Res.*, 99, 14415–14428, doi:10.1029/94jd00483, 1994.
- Liang, X., Wood, E. F., and Lettenmaier, D. P.: Surface soil moisture parameterization of the VIC-2L model: Evaluation and modification, *Global Planet. Change*, 13, 195–206, doi:10.1016/0921-8181(95)00046-1, 1996.
- Lockart, N., Kavetski, D., and Franks, S. W.: On the recent warming in the Murray–Darling Basin: land surface interactions misunderstood, *Geophys. Res. Lett.*, 36, L24405, doi:10.1029/2009GL040598, 2009.
- Lockart, N., Kavetski, D., and Franks, S. W.: On the recent warming in the Murray–Darling Basin: Land surface interactions misunderstood, *Geophys. Res. Lett.*, 36, L24405, doi:10.1029/2009GL040598, 2009.
- McMahon, T. A., Peel, M. C., and Karoly, D. J.: Assessment of precipitation and temperature data from CMIP3 global climate models for hydrologic simulation, *Hydrol. Earth Syst. Sci.*, 19, 361–377, doi:10.5194/hess-19-361-2015, 2015.
- McVicar, T. R., Van Niel, T. G., Li, L. T., Roderick, M. L., Rayner, D. P., Ricciardulli, L., and Donohue, R. J.: Wind speed climatology and trends for Australia, 1975–2006: Capturing the stilling phenomenon and comparison with near-surface reanalysis output, *Geophys. Res. Lett.*, 35, L20403, doi:10.1029/2008GL035627, 2008.
- Meinshausen, M., Smith, S. J., Calvin, K., Daniel, J. S., Kainuma, M. L. T., Lamarque, J. F., Matsumoto, K., Montzka, S. A., Raper, S. C. B., Riahi, K., Thomson, A., Velders, G. J. M., and van Vuuren, D. P. P.: The RCP greenhouse gas concentrations and their extensions from 1765 to 2300, *Climatic Change*, 109, 213–241, doi:10.1007/s10584-011-0156-z, 2011.
- Milly, P. C. D., Dunne, K. A., and Vecchia, A. V.: Global pattern of trends in streamflow and water availability in a changing climate, *Nature*, 438, 347–350, 2005.
- Moriasi, D. N., Arnold, J. G., Van Liew, M. W., Bingner, R. L., Harmel, R. D., and Veith, T. L.: Model evaluation guidelines for systematic quantification of accuracy in watershed simulations, *T. ASABE*, 50, 885–900, 2007.
- Moss, R. H., Edmonds, J. A., Hibbard, K. A., Manning, M. R., Rose, S. K., van Vuuren, D. P., Carter, T. R., Emori, S., Kainuma, M., Kram, T., Meehl, G. A., Mitchell, J. F. B., Nakicenovic, N., Riahi, K., Smith, S. J., Stouffer, R. J., Thomson, A. M., Weyant, J. P., and Wilbanks, T. J.: The next generation of scenarios for climate change research and assessment, *Nature*, 463, 747–756, doi:10.1038/nature08823, 2010.
- Murray, S. J., Foster, P. N., and Prentice, I. C.: Evaluation of global continental hydrology as simulated by the Land-surface Processes and eXchanges Dynamic Global Vegetation Model, *Hydrol. Earth Syst. Sci.*, 15, 91–105, doi:10.5194/hess-15-91-2011, 2011.
- Murray, S. J., Foster, P. N., and Prentice, I. C.: Future global water resources with respect to climate change and water withdrawals as estimated by a dynamic global vegetation model, *J. Hydrol.*, 448–449, 14–29, doi:10.1016/j.jhydrol.2012.02.044, 2012.
- Murray, S. J., Watson, I. M., and Prentice, I. C.: The use of dynamic global vegetation models for simulating hydrology and the potential integration of satellite observations, *Prog. Phys. Geogr.*, doi:10.1177/0309133312460072, 2013.
- Nemani, R. R., Keeling C. D., Hashimoto, H., Jolly, W. M., Piper, S. C., Tucker, C. J., Myneni, R. B., and Running, S. W.: Climate-driven increases in global terrestrial net primary production from 1982 to 1999, *Science*, 300, 1560–1563, 2003.
- O’Grady, A. P., Carter, J. L., and Bruce, J.: Can we predict groundwater discharge from terrestrial ecosystems using existing eco-hydrological concepts?, *Hydrol. Earth Syst. Sci.*, 15, 3731–3739, doi:10.5194/hess-15-3731-2011, 2011.
- Obrist, D. and Arnone, J. A.: Increasing CO<sub>2</sub> accelerates root growth and enhances water acquisition during early stages of development in *Larrea tridentate*, *New Phytol.*, 159, 175–184, doi:10.1046/j.1469-8137.2003.00791.x, 2003.
- Palmer, A. R., Fuentes, S., Taylor, D., Macinnis-Ng, C., Zeppel, M., Yunusa, I., and Eamus, D.: Towards a spatial understanding of water use of several land-cover classes: an examination of relationships amongst pre-dawn leaf water potential, vegetation water use, aridity and MODIS LAI, *Ecophysiology*, 3, 1–10, doi:10.1002/eco.63, 2010.
- Peel, M. C. and Blöschl, G.: Hydrological modelling in a changing world, *Prog. Phys. Geogr.*, 35, 249–261, doi:10.1177/0309133311402550, 2011.
- Piao, S., Friedlingstein, P., Ciais, P., de Noblet-Ducoudré, N., Labat, D., and Zaehle, S.: Changes in climate and land use have a larger direct impact than rising CO<sub>2</sub> on global river runoff trends, *P. Natl. Acad. Sci. USA*, 104, 15242–15247, doi:10.1073/pnas.0707213104, 2007.
- Potter, N. J. and Chiew, F. H. S.: An investigation into changes in climate characteristics causing the recent very low runoff in the

- southern Murray–Darling Basin using rainfall–runoff models, *Water Resour. Res.*, 47, W00G10, doi:10.1029/2010WR010333, 2011.
- Roderick, M. L. and Farquhar, G. D.: A simple framework for relating variations in runoff to variations in climatic conditions and catchment properties, *Water Resour. Res.*, 47, W00G07, doi:10.1029/2010WR009826, 2011.
- Scheiter, S., Langan, L., and Higgins, S. I.: Next-generation dynamic global vegetation models: learning from community ecology, *New Phytol.*, 198, 957–969, 2013.
- Schenk, H. J. and Jackson, R. B.: The global biogeography of roots, *Ecol. Monogr.*, 72, 311–328, 2002.
- Taylor, K. E., Stouffer, R. J., and Meehl, G. A.: An overview of CMIP5 and the experiment design, *B. Am. Meteorol. Soc.*, 93, 485–498, doi:10.1175/BAMS-D-11-00094.1, 2012.
- Teng, J., Chiew, F. H. S., Vaze, J., Marvanek, S., and Kirono, D. G. C.: Estimation of climate change impact on mean annual runoff across Continental Australia using Budyko and Fu equations and hydrological models, *J. Hydrometeorol.*, 13, 1094–1106, 2012a.
- Teng, J., Vaze, J., Chiew, F. H. S., Wang, B., and Perraud, J.-M.: Estimating the relative uncertainties sourced from GCMs and hydrological models in modeling climate change impact on runoff, *J. Hydrometeorol.*, 13, 122–139, doi:10.1175/JHM-D-11-058.1, 2012b.
- Tesemma, Z. K., Wei, Y., Western, A. W., and Peel, M. C.: Leaf area index variation for cropland, pasture and tree in response to climatic variation in the Goulburn–Broken catchment, Australia, *J. Hydrometeorol.*, 15, 1592–1606, doi:10.1175/JHM-D-13-0108.1, 2014.
- Thornton, P. E. and Running, S. W.: An improved algorithm for estimating incident daily solar radiation from measurements of temperature, humidity, and precipitation, *Agr. Forest Meteorol.*, 93, 211–228, 1999.
- Uddling, J., Teclaw, R. M., Kubiske, M. E., Pregitzer, K. S., and Ellsworth, D. S.: Sap flux in pure aspen and mixed aspen–birch forests exposed to elevated concentrations of carbon dioxide and ozone, *Tree Physiol.*, 28, 1231–1243, 2008.
- Vaze, J. and Teng, J.: Future climate and runoff projections across New South Wales, Australia: results and practical applications, *Hydrol. Process.*, 25, 18–35, doi:10.1002/hyp.7812, 2011.
- Vaze, J., Post, D. A., Chiew, F. H. S., Perraud, J. M., Viney, N. R., and Teng, J.: Climate non-stationarity – validity of calibrated rainfall–runoff models for use in climate change studies, *J. Hydrol.*, 394, 447–457, doi:10.1016/j.jhydrol.2010.09.018, 2010.
- Verdon-Kidd, D. C. and Kiem, A. S.: Nature and causes of protracted droughts in southeast Australia: comparison between the Federation, WWII, and Big Dry droughts, *Geophys. Res. Lett.*, 36, L22707, doi:10.1029/2009GL041067, 2009.
- Vuuren, D. P., Edmonds, J., Kainuma, M., Riahi, K., Thomson, A., Hibbard, K., Hurtt, G. C., Kram, T., Krey, V., Lamarque, J.-F., Masui, T., Meinshausen, M., Nakicenovic, N., Smith, S. J., and Rose, S. K.: The representative concentration pathways: an overview, *Climatic Change*, 109, 5–31, 2011.
- Warren, J. M., Norby, R. J., and Wullschleger, S. D.: Elevated CO<sub>2</sub> enhances leaf senescence during extreme drought in a temperate forest, *Tree Physiol.*, 31, 117–130, doi:10.1093/treephys/tpr002, 2011.
- Western, A. W., Grayson, R. B., and Green, T. R.: The Tarrawarra project: high resolution spatial measurement, modelling and analysis of soil moisture and hydrological response, *Hydrol. Process.*, 13, 633–652, 1999.
- White, D. A., Battaglia, M., Mendham, D. S., Crombie, D. S., Kinal, J. O. E., and McGrath, J. F.: Observed and modelled leaf area index in Eucalyptus globulus plantations: tests of optimality and equilibrium hypotheses, *Tree Physiol.*, 30, 831–844, doi:10.1093/treephys/tpq037, 2010.
- Wullschleger, S. D., Epstein, H. E., Box, E. O., Euskirchen, E. S., Goswami, S., Iversen, C. M., Kattge, J., Norby, R. J., van Bodegom, P. M., and Xu, X.: Plant functional types in Earth System Models: past experiences and future directions for application of dynamic vegetation models in high-latitude ecosystems, *Ann. Bot.-London*, 114, 1–16, 2014.
- Yapo, P. O., Gupta, H. V., and Sorooshian, S.: Multi-objective global optimization for hydrologic models, *J. Hydrol.*, 204, 83–97, doi:10.1016/S0022-1694(97)00107-8, 1998.
- Yu, M., Wang, G., Parr, D., and Ahmed, K.: Future changes of the terrestrial ecosystem based on a dynamic vegetation model driven with RCP8.5 climate projections from 19 GCMs, *Clim. Change*, 127, 257–271, doi:10.1007/s10584-014-1249-2, 2014.
- Zhao, F., Chiew, F. H. S., Zhang, L., Vaze, J., Perraud, J.-M., and Li, M.: Application of a macroscale hydrologic model to estimate streamflow across southeast Australia, *J. Hydrometeorol.*, 13, 1233–1250, doi:10.1175/jhm-d-11-0114.1, 2012a.
- Zhao, F. F., Xu, Z. X., and Zhang, L.: Changes in streamflow regime following vegetation changes from paired catchments, *Hydrol. Process.*, 26, 1561–1573, doi:10.1002/hyp.8266, 2012b.
- Zhao, R. J., Zhuang, Y. L., Fang, L. R., Liu, X. R., and Zhang, Q. S.: The Xinanjiang Model, *Hydrological Forecasting Proceedings Oxford Symposium*, IAHS Press, 571 pp., 1980.